J Exp Biol Advance Online Articles. First posted online on 16 November 2016 as doi:10.1242/jeb.145615
Access the most recent version at http://jeb.biologists.org/lookup/doi/10.1242/jeb.145615

Ammonia excretion in the marine polychaete *Eurythoe complanata* (Annelida)

Daniel Thiel[2,3#)], Maja Hugenschütt[2#)], Heiko Meyer[2)], Achim Paululat[2)], Alex R. Quijada-Rodriguez[1], Günter Purschke[2)], and Dirk Weihrauch[1*)]

[1)]University of Manitoba, Winnipeg, Manitoba, Canada

[2)]University of Osnabrueck, Fachbereich Biologie, Department of Zoology, 49069 Osnabrueck, Germany

[3)]present address: Sars International Centre for Marine Molecular Biology, Thormøhlensgate 55,

5008 Bergen, Norway

# These authors contributed equally

*corresponding author

Dirk.Weihrauch@ad.umanitoba.ca

Summary statement: Ammonia excretion in a common marine burrowing polychaete occurs *via* dentrically branched and well vascularized branchiae, which exhibit high abundance of 3 AMTs and a Rh-protein. Here the excretion mechanism was investigated.

Key words: AMTs, gill morphology, V-ATPase, cAMP, acid-base regulation, HEA

Abstract

Ammonia is a toxic waste product from protein metabolism and needs to be either converted into less toxic molecules or, in the case of fish and aquatic invertebrates, excreted directly as is. In contrast to fish, very little is known regarding the ammonia excretion mechanism and the participating excretory organs in marine invertebrates. In the current study ammonia excretion in the marine burrowing polychaete *Eurythoe complanata* was investigated. As a potential site for excretion the 100-200 micrometer long, 30-50 micrometer wide and up to 25 micrometer thick dentrically branched, well ventilated and vascularized branchiae (gills) were identified. In comparison to the main body, the branchiae showed considerably higher mRNA expression levels of Na^+/K^+-ATPase, V-type H^+-ATPase, cytoplasmatic carbonic anhydrase (CA-2), a Rhesus-like protein, and three different AMTs. Experiments on the intact organism revealed that ammonia excretion did not occur *via* apical ammonia trapping, but was regulated by a basolateral localized V-type H^+-ATPase, carbonic anhydrase and intracellular cAMP levels. Interestingly, the V-type H^+-ATPase seems to play a role in ammonia retention. A one week exposure to 1 mmol l^{-1} NH_4Cl (HEA) did not cause a change in ammonia excretion rates, while, the 3 branchial expressed AMTs were in tendency down-regulated. This indicates a shift of function in the branchial ammonia excretion processes under these conditions.

Introduction

Ammonia (in this study NH_3 refers to gaseous ammonia, NH_4^+ to ammonium ions, and ammonia to the sum of both) is a toxic waste product from protein metabolism and needs to be either detoxified into less toxic molecules or rapidly excreted to avoid detrimental accumulation in the body fluids (Larsen et al., 2014). For instance, in the shrimp *Penaeus stylirostris* elevated ammonia levels reduced the total number of immune active haemocytes (Le Moullac and Haffner, 2000) and in lobster and crayfish exposure to ammonia disrupts ionoregulatory functions (Harris et al., 1998; Young-Lai et al., 1991). For further information on toxic effects of ammonia in other animals including vertebrates please refer to Larsen et al. 2014.

With very few exceptions aquatic species such as teleost fish (Weihrauch et al., 2009; Wright and Wood, 2009), fully aquatic amphibians (Cragg et al., 1961; Fanelli and Goldstein, 1964; Wood et al., 1989) and virtually all aquatic invertebrates investigated so far are ammonotelic (Larsen et al., 2014; Wright, 1995), excreting the majority of their nitrogenous waste in the form of ammonia directly into the environment. Most of the ammonia is usually excreted *via* the gas-exchanging and ion-regulating branchiae (gills), well documented for fish and decapod crabs (Weihrauch and O'Donnell, 2015; Weihrauch et al., 2009; Wright and Wood, 2009). If classic branchiae are absent, ammonia is excreted through other appendices such as the anal papillae found in some aquatic insect larvae (Donini and O'Donnell, 2005; Weihrauch et al., 2011). In addition, the skin (epidermal tissue) plays an import role in the excretion process when appendices are absent as reported for some amphibians such as the African clawed frog *Xenopus laevis* and the neotenous newt, *Necturus maculosus* (Cruz et al., 2013; Fanelli and Goldstein, 1964), but also for leeches (Quijada-Rodriguez et al., 2015), planarians (Weihrauch et al., 2012) and nematodes (Adlimoghaddam et al., 2015).

The actual transepithelial ammonia excretion mechanism varies between tissues and species but usually involves a basolateral Na^+/K^+-ATPase (NKA), which actively transports NH_4^+ in replacement for K^+ ions from the body fluids into the epithelial cell (Masui et al., 2002; Quijada-Rodriguez et al., 2015; Weihrauch et al., 1998) and a Rh-protein which mediates basolateral ammonia transport (Adlimoghaddam et al., 2015; Nakada et al., 2007; Weihrauch et al., 2009). Further evidence is available suggesting that in freshwater organisms the exit of cellular ammonia occurs *via* apically localized Rh-proteins, a process energized by a co-localized V-type H^+-ATPase (HAT) that acidifies the apical unstirred boundary layer and thereby generating an outwardly directed partial pressure gradient for NH_3 (ΔP_{NH3}). This process might be supported by a co-localized Na^+/H^+-exchanger (NHE). The catalytic action of the carbonic anhydrase provides protons in this system (Weihrauch et al., 2012; Wright and Wood, 2009). For pH-buffered environments such as seawater or soil also a vesicular ammonia excretion mechanism has been proposed. Evidence suggested that in this mechanism ammonia is trapped in acidified vesicles, which are then transported along the microtubule network to the apical membrane of the epithelia cell, where NH_4^+ is excreted *via* exocytosis (Adlimoghaddam et al., 2015; Weihrauch et al., 2002).

Very limited information exists regarding the ammonia excretion mechanism or the actual site of excretion in marine polychaetous annelids. However, all marine polychaetes studied so far appear to be ammonotelic. For *Nereis succinea* and *Nereis virens* an active excretion was shown which depends partially on the activity of the Na^+/K^+-ATPase (Mangum, 1978). The site of excretion however, is still speculative. In this context, it was suggested that besides the metanephridial system the intensely vascularized parapodia as a whole might play a role in this process (O'Donnell, 1997).

In order to identify the site and mechanism of ammonia excretion in marine polychaetes in more detail, whole animal transport studies, gene expression analyses and

microscopy techniques have been employed in a burrowing marine species, *Eurythoe complanata*, the Mexican fireworm. Our studies indicate that ventilated hand-glove-like appendices localized at the posterior base of the notopodia represent the "branchiae" and are likely an important site of ammonia excretion and gas exchange. Immunohistochemistry revealed further a basolateral localization of the V-type H^+-ATPase in this tissue; unexpectedly, the enzyme seems to be involved in ammonia retention rather than in excretory processes.

Material and Methods

Animals

Individuals of *Eurythoe complanata* were maintained in an established 350 liter seawater tank (salinity 32‰, 25°C) at natural light settings in the biology department of the University of Osnabrück. Two weeks before experimentation animals (ca. 10 gram fresh weight, gFW) obtained from the large tank were divided and transferred into three two-liter containers (placed within the big tank), which contained mussel grit and artificial seawater (ASW; REEF SALT, Aqua Medic GmbH, Bissendorf, Germany), adjusted 32‰ salinity and pH 8.2. Animals were fed three times/week with tropical fish food (Ultra LPS, Fauna Marine GmbH, Holzgartingen, Germany), but starved 12 hours before experimentation. Every 2nd day the water was replaced.

Excretion experiments

For all excretion experiments animals (ca. 0.3-0.4 g FW, 0.5-2 cm in length) were transferred into small glass containers filled with 4 ml freshly prepared artificial seawater (ASW) and ca. 3 gram of sterilized mussel grit as a hiding substrate. Experiments were performed in a darkened water bath (25ºC). After an initial equilibration period (30 min), the container was rinsed 2 times (washing step) with ASW and refilled with 4 ml of fresh ASW for the first sampling period (control). After the control sampling period, an experimental sampling period and a final, 2nd control sampling period followed. Between each sampling period (1 hour), a washing step was conducted. At the end of each sampling period, two samples of 1.9 ml were taken from the containers for later analysis. For the evaluation of the procedures, prior to each experimental treatment 5 individual animals were exposed to the experimental conditions (e.g. pH or pharmacological agents) to ensure full recovery after a 1 hour exposure period. As acetazolamide, 5-(N-Ethyl-N-isopropyl) amiloride (EIPA), KH7, and KM91104 needed to be dissolved in DMSO (final concentration 0.1%), DMSO was also added to ASW for the respective control steps. All solutions employing inhibitors were adjusted to pH 8.2 by HCl or NaOH. For pH exposure experiments ASW was adjusted to pH 6 and 9 with 5 mmol l^{-1} Trizma base and HEPES, respectively.

High environmental ammonia (HEA)

In a set of experiments to assess the polychaete's compensatory response to chronic (one week) and acute (one hour) high ammonia exposures, *E. complanata* were placed, into six separate two liter containers, filled with mussel grit and either ASW or ASW enriched with 1 mmol l^{-1} NH_4Cl (HEA, 25ºC, pH 8.2). Animals were fed every 2nd day while ASW was replaced daily to keep the conditions as constant as possible. Also here animals were starved

12 hours prior experimentation. For all experiments, animals were taken randomly from the respective tanks.

Ammonia determination

Ammonia contents of ASW samples were measured using a gas-sensitive NH_3 electrode (Orion 9512 from Thermo Scientific, Cambridgeshire, England) connected to a digital mV/pH meter, following the procedure established by Weihrauch et al. (1998). All samples, were diluted 1:4 with ion-free water. Solutions for the standard curve were made according to the specific composition of the respective samples (e.g. pH or pharmacological agent), containing a range between 10 and 50 µmol l^{-1} NH_4Cl. Measurements were highly accurate with $R^2 \geq 0.99$.

Immunohistochemistry and Western blot

Animals were anesthetized using an isotonic solution of $MgCl_2$ (approx. 8% $MgCl_2*6H_2O$ w/v) in distilled water and after being immotile fixed in 4% paraformaldehyde in phosphate-buffered saline (PBS: 140 mmol l^{-1} NaCl, 6.5 mmol l^{-1} KCl, 2.5 mmol l^{-1} Na_2HPO_4, 1.5 mmol l^{-1} KH_2PO_4, 12% Sucrose, pH 7.4, 4°C, 2.5 h). After fixation specimens were rinsed in PBST (PBS + 0.1% Tween) for 2 h or overnight. Prior to immunolabeling, specimens were dissected and single parapodia or segments were further processed. To increase permeability they were treated with collagenase for 1.5 h (1000 U/ml collagenase Type VII from Sigma in 1 mmol l^{-1} $CaCl_2$, 0.1 % Triton X-100, 0.1 M Tris/HCl buffer pH 7.5) followed by PBST + 1% Tween and 1% TritonX-100 for 2 h. After rinsing with PBST specimens were incubated with PBST containing 0.1% BSA (bovine serum albumin) for 1 h, rinsed in PBST and incubated with primary antibodies for 2-4 d at 4°C. Primary antibodies were mouse anti-

acetylated α-tubulin (monoclonal, Sigma-Aldrich, Heidelberg, Germany, dilution 1:1.000) and guinea pig anti-V-ATPase (polyclonal, subunit B specific, dilution 1:100, (Weng et al., 2003)) Following washing (3x in PBST, 20 min each), secondary antibodies were applied for 2-3 d at 4°C (depending on the respective first antibodies either goat anti-mouse, Cy2 conjugated, goat anti-rabbit, Cy2 conjugated, goat anti-rabbit, Cy3 conjugated or goat anti-guinea pig, Cy 3 conjugated, Dianova, Hamburg, Germany, dilution 1:100). After being rinsed several times and washed in PBST overnight, specimens were mounted in Fluoromount (Southern Biotech, Birmingham, USA). For visualizing the musculature, specimens were incubated in fluorescein isothiocyanate-labelled phalloidin for 1 h (100 µg / 5ml EtOH; diluted 1:50 in PBS) and washed and embedded as described above. Confocal images were captured with a LSM 5 Pascal confocal microscope (Zeiss, Jena, Germany). Z-stacks are displayed as maximum projections if not stated otherwise. Specificity of immunoreactivity was controlled by incubating specimens in the same manner, but omitting the primary antibodies.

Western blots were done essentially as described earlier (Panz et al., 2012). Subsequent to homogenization (glass-teflon homogenizer) and boiling (3 min, 99°C), total protein extracts (10μg/lane) were separated by SDS-PAGE (17%) and transferred to nitrocellulose membranes (Carl Roth, Karlsruhe, Germany). Primary antibodies (anti-V-ATPase, polyclonal from guinea pig, subunit B specific, (Weng et al., 2003) were applied at a dilution of 1:500, and secondary antibodies (goat anti-guinea pig IgG (whole molecule)-alkaline phosphatase conjugate, Sigma-Aldrich) at a dilution of 1:10,000.

Electron microscopy

For electron microscopy specimens were fixed in a phosphate-buffered mixture of sucrose, picric acid, glutaraldehyde and paraformaldehyde (SPAFG) (Ermak and Eakin, 1976) for 2.5 h at 4°C and rinsed in phosphate buffer adjusted to the osmolarity of seawater(4°C, pH 7.2, 12% sucrose). Post fixation occurred in 1% OsO_4 for 1 h (phosphate buffered as above) and dehydrated in a graded ethanol series. For SEM, specimens were then critical point dried with CO_2 and mounted on aluminum stubs, sputter coated with gold-palladium and examined with in a Zeiss Auriga scanning electron microscope. For TEM, after dehydration specimens were step wise transferred into the intermedium propylene oxide (EtOH and propylene oxide 1:1, pure propylene oxide). Infiltration was in a mixture of the embedding medium and propylene oxide (1:3) overnight. Specimens were embedded in a mixture of Araldite and PolyBed 812. Polymerization was carried out at 60°C for 72h. Ultrathin sections of the branchiae (70 nm) were made using a diamond knife on a Leica Ultracut E or Leica EM UC 6. Sections were mounted on single slot grids, contrasted with 2% uranyl acetate and 0.5% lead citrate for 30 and 20 min, respectively, in a Nanofilm Surface Analysis ultrastainer. Sections were examined in Zeiss EM 902A transmission electron microscope operated at 50 or 80 kV. Micrographs were taken using a 4K CCD camera, TRS, Moorenweis, Germany. Images were further processed using Image SP, Adobe Photoshop © and Illustrator ©.

Quantitative PCR (qPCR)

Total RNA extractions were accomplished using Trizol (Invitrogen, Carlsbad, CA, USA) in an RNase-free environment, followed by DNase digestion using DNAse 1 (Invitrogen, Carlsbad, CA, USA). Branchiae from control and HEA exposed animals (see above) were isolated as well as bodies, which were stripped of their branchiae. Quality of total RNA was

checked by gel electrophoresis and by Nano-drop measurement assessing 260:280 and 230:280 ratio. Before transcription, RNA was treated with DNase I (Invitrogen, Carlsbad, CA, USA), followed by PCR (40 cycles) targeting GAPDH (see table 1) to verify the absence of genomic DNA. Complementary DNA was synthesized using MonsterScript™ (Epicentre, Madison, USA). Quantitative PCR was performed in a 2 step protocol with the annealing temperature set to 57°C. Prior to qPCR, a regular PCR was performed employing qPCR primers for all target genes. The resulting single PCR products were sequenced to confirm specificity. For the standard curve, defined amounts of amplified PCR products were used. GAPDH served as the reference gene as mRNA expression levels were similar between tissues and did not change upon treatments (data not shown). Primer sequences, PCR product sizes and the references gene-sequences accession numbers are provided in table 1.

Phylogenetic analysis of Rhesus glycoproteins and Ammonium transporters (AMTs)

The Rh protein and AMT data set contained 39 protein sequences. Amino acid sequences were aligned by MUSCLE alignment in MEGA 6. The most appropriate phylogenetic analysis model from 56 available models was determined utilizing the Mega 6 best model function. Phylogenetic analysis of MUSCLE aligned sequences was then performed in MEGA 6 using the maximum likelihood method with the LG + four categories of gamma substitution rates + invariable sites model and Nearest Neighbor Interchange (NNI) Heuristic Method. Bootstrap values were determined from 1000 bootstrap replicates.

Statistics

In this study, each N value represents the combined pool of polychaetes with a mass of ca. 0.3-0.4 g FW for transport experiments and ca. 0.3 mg of total pooled tissues for RNA isolation. Values from all experiments specified as the mean +/− standard error of the mean

(SEM). Significance ($p \leq 0.05$) between controls and treatments are indicated by "*". Statistical methods for the individual experiments are provided in the figure legends.

Results

The ammonia excretion rate in *Eurythoe complanata* under control conditions (pH, 8.2) accounted for 0.38 ± 0.026 µmol gFW^{-1} h^{-1} (n=39). The excretion was constant over a time period of at least 3 hours however, when mussel grit was omitted from the test containers, excretion rates increased by ca. 55.3% (n=4, data not shown). This was most likely stress related, as prolonged rearing on plain glass (no hiding possibilities) led to a loss of their bristles. In order to evaluate whether the excretion rates depended on the environmental pH, whole animals were either placed into artificial SW buffered to pH 8.2 (control), pH 6, or pH 9 for 1 hour. When exposed to seawater adjusted to pH 6, the excretion rate was not different from controls (Fig. 1A). In contrast, when exposed to pH 9 excretion rates decreased by approximately 40%. When after 1 hour of exposure the animals were placed back into control media (pH 8.2), increased levels of excretion were observed, suggesting a release of accumulated ammonia from the blood (Fig. 1B).

Mode of ammonia excretion

Since it was assumed that at least part of the animals' ammonia excretion occurs over epithelia directly facing the environment, in the next series of experiments animals were exposed to a variety of different pharmacological agents to gather the first information regarding the nature of the excretion mechanism. Application of 5 µmol l^{-1} of the V-type H^+-ATPase (HAT) inhibitor KM91104 and 2 mmol l^{-1} acetazolamide, an inhibitor of the

carbonic anhydrase (CA), caused a significant increase of the excretion rates by approximately 1.2 and 1.5-fold, respectively (Fig. 2A). Exposure to 100 µmol l^{-1} EIPA, a blocker of Na^+/H^+-exchangers, and 0.5 mmol l^{-1} colchicine, a destabilizer of the microtubule network, had no effect on ammonia excretion rates in the polychaete (Fig. 2A). In the next series of experiments it was tested whether ammonia excretion is influenced by cAMP, a secondary messenger. Ammonia excretion was significantly activated by 10 µmol l^{-1} KH7, a selective inhibitor of the soluble adenylyl cyclase, but partly inhibited by elevated intracellular cAMP levels induced by application of either 25 µmol l^{-1} 8-bromo-cAMP or 1 mmol l^{-1} of the phosphodiesterase inhibitor theophylline (Fig. 2B). After the wash-out step in the 3rd sampling period, the effects of KM91104, acetazolamide, 8-bromo-cAMP, and KH7 continued, while omitting theophylline caused a partial return to the initial control excretion rates (data not shown).

Characterization of the branchiae (gills)

In *E. complanata* a pair of branchiae are present on each segment from the anterior end throughout the entire body. The branchiae are situated at the notopodia close to the dorsal cirrus and immediately behind the bundle of notochaetae (Fig. 3, B).

The branchiae are dentrically branched and comprise a dorsal and a ventral tuft of flattened branches (Fig. 3C). These branches are about 100-200 µm long, 30-50 µm wide and up to 25 µm thick. Each branch is supplied with a band of densely arranged motile cilia at its narrow edges (Fig. 3D). In living animals the cilia are continuously beating when observed under a light microscope. In addition, there are several tufts of short cilia present on the flattened surface of the branchiae (Fig. 3D). These cilia are immotile and belong to primary receptor cells; innervation and receptor cells will be described in a forthcoming paper (Purschke et al.

unpubl. obs.). The branchiae are primarily epidermal structures comprising only a few cell types including unciliated supportive cells and ciliated cells forming the ciliary bands mentioned above (Fig. 3E). The epidermis is covered by a collagenous cuticle which is thinner than the cuticle on the trunk (Fig. 3E; details will be described elsewhere). The branchiae are supplied with a well-developed musculature comprising longitudinal and circular fibers (Fig. 3F), which largely follow the course of the main vessels. The branchiae are well vascularized and the main vessels give rise to numerous branches, which extend close to the surface (Fig. 3E, G). So the blood is covered by epidermal cells less than 1 µm thick. Due to the presence of blood vessels the branchiae appear reddish in color in living animals or fresh fixed material. Endothelial cells are lacking and the blood spaces are only lined by the extracellular matrix (ECM) separating adjacent epithelial cells (Fig. 3G). The branchiae are covered by a comparatively thin collagenous cuticle (1.8 µm ± 0.3 µm), which is traversed by numerous epidermal microvilli. The microvilli have a diameter of ca. 35 nm with 18 ± 4 microvilli μm^{-2} surface (Fig. 3E, G).

To further verify that the described branchiae are a potential site for ammonia excretion, it was assessed whether transcripts of proteins commonly found to be responsible for gas exchange and ammonia excretion are expressed. For this the branchiae were isolated and mRNA expression levels of key-transporters/enzymes compared to expression levels in the main body that has been stripped of the branchiae. The results showed that carbonic anhydrase isoform 2 (CA-2, cytoplasmatic isoform), Na^+/K^+-ATPase (α-subunit, NKA), and V-type H^+-ATPase (subunit B, HAT) were approx. 11, 4, and 4 times higher expressed in the

branchiae compared to the remaining body, respectively (Fig. 4A). One Rh-protein was identified in the branchiae and named EcRhp1b (GenBank accession #: KX421088). Note, Ec stands for the species name, while Rhp1 stands for the invertebrate primitive Rh-protein cluster. EcRhp1b revealed a 4-fold higher mRNA abundance in this tissue compared to the body (Fig. 4B). All absolute mRNA expression values of control polychaetes can be found in table 2. In addition to the Rh-protein, three transcripts were identified coding for proteins clustering all together with ammonia transporters (AMTs) from plants, methylamine permeases (Meps) from fungi and AMTs from other invertebrates (Fig. 5). These putative ammonia transporters were named EcAMT1 (GenBank accession #: KX458239), EcAMT3 (Genbank accession #: KX421089) and EcAMT4 (Genbank accession #: KX421090), according to their sequence similarities to AMTs expressed in *Caenorhabditis elegans*. All AMTs exhibited higher abundance in the branchiae when compared to the main body with approximately 58, 6, and 12 times higher relative mRNA expression for EcAMT1, EcAMT3 and EcAMT4, respectively (Fig. 4B). Note, as seen in table 2, qPCR revealed that transcript levels of EcAMT4 are extraordinary high in the branchiae, with approximately 8 and 4 times higher absolute abundance compared to transcript levels detected for Na^+/K^+-ATPase (α-subunit) and EcRhp1b, respectively.

Localization of V-type H^+-ATPase

Since the V-type H^+-ATPase is in general a key player in ammonia transport processes, presence and localization of the multi-subunit enzyme within the branchiae was analyzed by means of immunohistochemistry. In this effort, we utilized polyclonal antibodies raised against the subunit B of the tobacco hornworm *Manduca sexta* V-type H^+-ATPase (Weng et al., 2003). In order to confirm specificity of the antiserum in *E. complanata*, Western blots were performed with total protein extracts isolated from adult animals. As depicted in figure 6A, application of the respective antiserum resulted in distinct detection of a single protein

with a molecular mass of about 55 kDa, which corresponds quite well to the expected subunit B mass of 56 kDa (Weng et al., 2003). These data strongly indicate that the applied antiserum specifically detects subunit B of the *E. complanata* V-type H^+-ATPase. Utilizing the respective antiserum in tissue staining revealed further that within the branchiae the V-type H^+-ATPase localizes to basolateral membranes of the single-cell-layered epithelium. In addition to this localization, a second signal is apparent in a patchy manner within the cytoplasm, presumably representing vesicles containing the V-type H^+-ATPase (Fig. 6B).

Effects of high environmental ammonia (HEA)

In the next series of experiments animals were exposed for 1 week either to control seawater (pH 8.2) or to seawater enriched with 1 mmol l^{-1} NH_4Cl (HEA, pH 8.2) to assess potential changes in ammonia excretion rates and mRNA expression levels of key-proteins involved in the transport mechanism.

When control animals were exposed acutely for 1 hour to HEA, the animal's ammonia excretion reversed into an ammonia uptake. After re-exposure to ammonia-free seawater ammonia excretion was reestablished, however with a significant higher rate compared to the initial control excretion value (Fig. 7A). When animals exposed to HEA for 1 week were placed in ammonia free SW the excretion rates were 1.94 ± 0.14 µmol gFW^{-1} h^{-1} about 3 times as high as rates measured in control animals (0.75 ± 0.06 µmol gFW^{-1} h^{-1}). Notable, when animals were subsequently exposed to HEA (acclimation media), excretion rates were with 0.75 ± 0.32 µmol gFW^{-1} h^{-1} basically identical to the excretion rates measured in control animals excreting in ammonia-free seawater (Fig. 7A, 7B). Chronic exposure to HEA caused also an increase in mRNA levels in the body (stripped from branchiae) for NKA (α-subunit), CA-2, and in tendency also EcAMT1, whereas mRNA expression levels of HAT (subunit B),

EcRhp1b, EcAMT3, and EcAMT4 remained unchanged. Also in the branchiae HEA caused a differential expression pattern of some target genes. Whereas relative mRNA expression levels of NKA and EcRhp1b did not change, HAT was in tendency up-regulated. CA-2 and all AMTs were in tendency down-regulated compared to expression levels found in the branchiae of control animals (Fig. 8).

Discussion

The branchiae

Besides a general diversity in terms of position, external structure and occurrence of branchiae in annelids, certain common characters become obvious which likewise can be observed in the amphinomid *E. complanata* (Gardiner, 1988; Rouse and Pleijel, 2001). Most polychaete branchiae studied so far are equipped with motile cilia, which are either arranged in bands, clusters or tufts effecting continuous and strong water currents (Gardiner, 1988). Likewise epidermis and cuticle are always thinner than in other parts of the body. It should be noted that the annelid cuticle is a soft, flexible, not a tight border and typically traversed by numerous microvilli (Hausen, 2005; Purschke et al., 2014). Mostly annelid branchiae are supplied with efferent and afferent vessels which give rise to some kind of connecting vessel and often blind-ending blood spaces extending deeply into the epidermal cells. Usually the distance between the blood spaces and the external medium has been reported to be as short as 1 µm but can exceed 7-10 µm (Gardiner, 1988). Other studies report thickness of epidermal cells covering the blood spaces in the same order than observed in the present investigation, which belong to the smallest diffusion distances reported so far, e. g. in *Diopatra neopolitana.* (Menendez et al., 1984). As typical for annelids and invertebrates, in general these vessels represent spaces in the ECM of adjacent epithelia (Fransen, 1988;

Westheide, 1997). The absence of a well-developed basal labyrinth system, usually characteristic of actively transporting cells, led certain authors to conclude that branchiae do not have additional functions such as osmoregulation or excretion (Gardiner, 1988; Storch and Alberti, 1978). Since a basal labyrinth system has not been observed either in *E. complanata* or in other annelids, additional studies were needed to clarify whether they have additional functions. Gene expression studies conducted in the current investigation support indeed the notion that ammonia excretion and acid-base regulation is at least partly accomplished by the branchiae in *E. complanata*. High branchial mRNA expression levels of Na^+/K^+-ATPase, V-type H^+-ATPase, CA-2 and a Rh-protein, all genes known to be involved in ammonia excretion and acid-base regulation (Larsen et al., 2014) as well as the observed ultrastructure of the tissue, which features traits of typical branchiae/gills of osmoconforming invertebrates (Gardiner, 1992; Smith, 1992), provide indirect but strong evidence for this assumption.

Particularly of interest was the identification and branchial expression of three AMTs, proteins best known to be the main transporters for NH_4^+ uptake in plant roots (Ludewig et al., 2002). Although, not shown so far to be expressed in vertebrates, transcriptome projects revealed that AMTs are expressed in invertebrates, clustering closer to the high affinity transporters (AMT1 family) found in plants, than to the fungal MEPs and bacterial AmtBs (Fig. 5). To the authors' knowledge only two studies, both on mosquitoes, investigated the function and role of AMTs in invertebrate species. While a functional study on adult *Anopheles gambiae* strongly suggested that AMTs in invertebrates mediate the transport of NH_4^+ (Pitts et al., 2014), a physiological study on the anal papillae of yellow fever mosquito *Aedes aegypti* larvae showed the importance of AMTs in the ammonia excretion process. Immunohistochemistry further revealed a basal localization of the AMT in the epithelium of the anal papillae (Chasiotis et al., 2016). As mentioned above, in *E. complanata* transcripts of

three different AMTs have been identified within the branchiae, exhibiting among each other vastly different mRNA expression levels. Information regarding their cellular localization require further studies however, one can expect presence of an AMT on either side of the gill epithelium due to its potential function as a pathway for NH_4^+. Moreover, with caution one could speculate that EcAMT4 is localized to the basolateral membrane, as its relative high expression level compared to the Rh-protein, is similar to what was found in the anal papillae of *A. aegypti* (Chasiotis et al., 2016). The overall importance of EcAMT4 is further underlined by its absolute mRNA expression level in the branchiae, which was considerably higher compared to transcript levels found for the gill energizing pump, Na^+/K^+-ATPase, but also the major acid-base regulatory protein, CA-2.

Working model for the branchial ammonia excretion mechanism

In order to provide a basis for future studies and discussions we integrated the gained information regarding the branchial ammonia excretion mechanism in *E. complanata* into a working model (Fig. 9). For this model it is assumed that NH_4^+ is transported from the blood into the branchial epithelial cells in an active manner by the $Na^+/K^+(NH_4^+)$-ATPase. While no direct evidence could be provided in this study due to lethality of ouabain treatment to *E. complanata*, this mechanism has been shown in other marine polychaetes namely, *Nereis succinea* and *Nereis virens*, but also for the ammonia transporting epithelia of many other vertebrates and invertebrates (Evans et al., 1989; Larsen et al., 2014; Mangum, 1978; Quijada-Rodriguez et al., 2015; Weihrauch et al., 1998). Further, NH_4^+ may also move into the cells driven by the negative intracellular potential *via* a basolateral localized AMT, possibly EcAMT4. It is, however also very possible that the basolateral AMT rather serves as a NH_4^+ back-flow valve to limit a cytoplasmatic overload, similar to epithelial basolateral K^+-channels (Riestenpatt et al., 1996). Respiratory CO_2 might enter the cells *via* a basolaterally localized Rh-protein, which has for physiological systems strongly been suggested to

function as a dual gas-channel, mediating the transport of NH_3 and CO_2 (Endeward et al., 2008; Kustu and Inwood, 2006; Perry et al., 2010; Soupene et al., 2004). Due to its high mRNA expression levels in the body, it is assumed that EcRhp1b is the basolateral localized "housekeeping" transporter, similar to CeRhr-1, identified in the nematode *Caenorhabditis elegans* (Adlimoghaddam et al., 2015; Adlimoghaddam et al., 2016). As described below, EcRhp1b might serve as a NH_3 back-flow channel, important for acid-base homeostasis (Fig 9A). It can however, not be excluded that the Rh-protein provides also an exit for NH_4^+ as recent studies demonstrated that at least some mammalian Rh-glycoproteins are capable to mediate the transport of both forms of ammonia (Caner et al., 2015). Apical exit of NH_4^+ is likely driven by the outwardly directed electrochemical gradient for NH_4^+ and probably mediated by an apical localized AMT. Apical ammonia trapping (acid trapping) *via* Rh-proteins, as suggested for ammonia excreting epithelia in freshwater invertebrates and fish (Larsen et al., 2014; Quijada-Rodriguez et al., 2015; Wright and Wood, 2009), is likely not of major importance of the excretory mechanisms in *E. complanata*. This is evident by the lack of an apical V-ATPase and the observed unaltered ammonia excretion rate, when animals were exposed to an environment that was buffered to pH 6, a condition that, considering a physiological intracellular pH between 7.3 and 7.8, established a considerable outwardly directed P_{NH3}. Moreover, due to the lack of inhibition upon application of colchicine, a vesicular microtubule-dependent ammonia excretion mechanism, as suggested functioning in gills of the green crab *Carcinus maenas* (Weihrauch et al., 2002) and the hypodermis in of the nematode *Caenorhabditis elegans* (Adlimoghaddam et al., 2015), is not assumed to be in place in *E. complanata*. In addition, the basolateral localized V-type H^+-ATPase, as well as the pharmacological experiments employing modulators of cellular cAMP levels suggest that the branchiae of *E. complanata* exhibit also a regulatory function that is set up to transport NH_3, in a secondary active manner, out of the cytoplasm back into the blood. The V-type H^+-

ATPase, localized in the basolateral membrane, likely generates a cytoplasm-to-blood directed P_{NH3} gradient by a steady acidification of the blood within the vessels in branchial tissue that consequently drives NH_3 out of the cell *via* EcRhp1b or simple membrane diffusion (Goldmann and Rottenberg, 1973). Supported by the reduced excretion rates after exposure to theophylline and 8-bromo-cAMP, activity of the V-type H^+-ATPase is here likely activated by intracellular cAMP as e.g. demonstrated for the assembly and activity of plasma membrane V-type H^+-ATPase in blowfly salivary glands (Dames et al., 2006) (Fig. 9A). Alternatively, intracellular cAMP may not directly activate V-type H^+-ATPase but instead signal for translocation of additional V-type H^+-ATPase containing cytoplasmic vesicles to fuse with the basolateral membrane to increase the abundance of this protein as seen in the gills of Pacific spiny dogfish *Squalus acanthias* L. (Tresguerres et al., 2010). Consequently, a reduction of cellular cAMP levels by inhibiting the soluble adenylyl cyclase (sAC) is thereby reducing amount of basolateral V-type H^+-ATPase and consequently a decrease of the acidification of the blood. (Fig. 9B). A blood directed ammonia transport was also observed in perfused gills of the marine cephalopod *Octopus vulgaris*, where hemolymph ammonia levels were maintained and adjusted by metabolically produced ammonia to approximately 300 µmol l^{-1} (Hu pers. communication), when plasma levels were below that value. Further a function of retaining ammonia in particular situations was also observed when *E. complanata* was exposed to a high environmental pH. Under this condition it would be physiologically meaningful to reduce NH_4^+ excretion and retain the acid-equivalent in order to maintain acid-base homeostasis. If animals were placed back into control seawater (pH of 8.2), excess ammonia was excreted at an increased rate to rid accumulated blood ammonia. Finally, high influx rates upon a short term exposure to elevated environmental NH_4Cl concentrations indicates further that the paracellular pathway for ammonia also plays a certain role in transepithelial ammonia fluxes.

As an alternative to the backflow hypothesis, it is plausible that the protons pumped into the blood by the V-type H^+-ATPase work to trap ammonia in the blood as NH_4^+. This action would thereby reduce NH_3 excretion into the cytoplasm of the cells rather than drive a backflow of NH_3 from cell to blood as proposed above. Here a reduction in NH_3 flux would essentially still aid in an ammonia retention as was also proposed in the ammonia backflow hypothesis above. In order to distinguish between these two hypothetical mechanism further studies will be required to localize transporters and determine intra- and extracellular pH/ammonia concentrations to assess the feasibility of ammonia backflow.

Exposure to high environmental ammonia (HEA)

As a burrowing animal it is likely that *E. complanata* experiences from time to time elevated environmental ammonia levels due to an accumulation of metabolically released ammonia while in the burrow (Weihrauch, 1999). Acute exposure to 1 mmol l^{-1} ammonia caused a rapid uptake of ammonia. That would be expected as the coelomic fluid of another marine polychaete, the lugworm *Arenicola marina* contains approximately 550 µmol l^{-1} ammonia (Reitze, 1989). Therefore during a 1 mmol l^{-1} ammonia exposure, an inwardly directed ammonia gradient would likely be present. Also other marine invertebrates usually have fairly low hemolymph/blood ammonia concentrations ranging between approximately 100 and 300 µmol l^{-1} as observed e.g. in crustaceans (Weihrauch et al., 2004), cephalopods (Hu, pers. communication) and horseshoe crabs (Hans, pers. communication). The influx might be facilitated also by a high epithelial conductance as directly shown for the gill epithelium in *Cancer pagurus* (Weihrauch, 1999). However, after a 7 day acclimation to HEA, *E. complanata* was capable of excreting ammonia at control rates. When exposed to regular seawater, excretion rates tripled, indicating that blood ammonia concentrations in HEA acclimated polychaetes are now above environmental levels. Since blood ammonia has not been assessed, this assumption is speculative but nevertheless supported by the fact that

transcript levels of several genes (NKA, CA-2, and in tendency EcAMT1 and EcAMT3) potentially involved in ammonia transport processes are up-regulated within the body. Since presumably now internal organs are exposed to elevated blood ammonia levels, a higher abundance of these genes might protect the body cells from toxic effects. Alternatively, the observed increase in mRNA expression in the body could be indicative of another ammonia transporting epithelia playing a greater role during HEA exposure such as the metanephiridia and/or intestine both previously shown in annelids to transport ammonia (Kulkarni et al., 1989; Tillinghast, 1967; Tillinghast et al., 2001). In contrast to the branchiae, both the intestine and metanephridia are not in direct contact with the environment and therefore maybe more readily capable of excreting ammonia unchallenged by the strong environmental ammonia gradient. Elevated transcript levels of an Rh-protein were also observed in various tissues of HEA (1 mmol l^{-1}, 2 weeks) acclimated Dungeness crabs *Metacarcinus magister*. Here hemolymph levels rose to nearly environmental concentrations (Martin et al., 2011). It is noteworthy that in HEA (1 mmol l^{-1} NH_4HCO_3) exposed marine pufferfish, after an initial ammonia uptake, excretion resumed after 12 hours to control rates, while plasma ammonia concentrations increased from approximately 300 µmmol l^{-1} to near environmental levels (Nawata et al., 2010).

Changes in transcript expression levels do not support the assumption that the observed ammonia excretion in HEA seawater was due to an activated/enhanced branchial excretion mechanism. In fact, with the exception of the V-type H^+-ATPase, which was in tendency up-regulated, the potential ammonia transporters EcAMT1, EcAMT3 and EcAMT4 were in tendency down-regulated. Anyhow, if the basolateral AMT serves, as speculated above, also as a NH_4^+ back-flow valve, to reduce an overload of intracellular ammonia, a down-regulation of this transporter would keep intracellular ammonia levels higher, promoting thereby excretion. However, as mentioned earlier, it could be that another ammonia

transporting tissue (e.g. metanephridia and/or intestine) is activated and the branchiae may reduce ammonia transport capabilities to prevent ammonia influx through branchial tissues. More mechanistic studies, as well was functional expression analysis for the Rh-proteins and all AMTs are required to make further statements regarding the ammonia excretion mechanism in HEA acclimated *E. complanata*.

Conclusion

The study of invertebrates in regard to their nitrogen excretion mechanism and tolerance towards environmental stressors has been neglected in the past, even in spite of their overall dominance (number of phyla and species) and ecological importance in the animal kingdom. By investigating marine invertebrates such as decapod crabs, cephalopods and, as in this case marine polychaetes, it has become obvious that ammonia has an important role as an acid-base equivalent in aquatic animals (Fehsenfeld and Weihrauch, 2012; Fehsenfeld and Weihrauch, 2016; Hu et al., 2013). Ammonia, which can actively be excreted or retained within the body fluids might very likely be crucial for blood pH homeostasis, particularly in animals exhibiting a very high ion-conductance of their surface epithelia such as marine invertebrates, where ammonia can easily leak out *via* the paracellular pathway into the environment.

Acknowledgements

We like to thank Dr. Helmut Wieczorek for providing the anti V-ATPase subunit B antiserum.

This work was supported by the “Incentive Award of the Faculty of Biology/Chemistry” (University of Osnabruck) to HM, and by grants from the German Research Foundation to AP and HM (SFB 944). AP received additional funding from the State of Lower-Saxony, Hannover, Germany (11-76251-99-15/12 (ZN2832)), AQ-R and DW were funded by NSERC.

References

Adlimoghaddam, A., Boeckstaens, M., Marini, A. M., Treberg, J. R., Brassinga, A.-K. and Weihrauch, D. (2015). Ammonia excretion in *Caenorhabditis elegans*: mechanism and evidence of ammonia transport of the Rh-protein CeRhr-1. *J Exp Biol* **218**, 675-683.

Adlimoghaddam, A., O'Donnell, M. J., Kormish, J., Banh, S., Treberg, J. R., Merz, D. and Weihrauch, D. (2016). Ammonia excretion in Caenorhabditis elegans: Physiological and molecular characterization of the rhr-2 knock-out mutant. *Comp Biochem Physiol A Mol Integr Physiol* **195**, 46-54.

Caner, T., Abdulnour-Nakhoul, S., Brown, K., Islam, M. T., Hamm, L. L. and Nakhoul, N. L. (2015). Mechanisms of ammonia and ammonium transport by rhesus-associated glycoproteins. *Am J Physiol Cell Physiol* **309**, C747-58.

Chasiotis, H., Ionescu, A., Misyura, L., Bui, P., Fazio, K., Wang, J., Patrick, M., Weihrauch, D. and Donini, A. (2016). An animal homolog of plant Mep/Amt transporters promotes ammonia excretion by the anal papillae of the disease vector mosquito, Aedes aegypti. *J Exp Biol* **219**, 1346-55.

Cragg, M. M., Balinsky, J. B. and Baldwin, E. (1961). A comparative study of nitrogen excretion in some amphibia and reptiles. *Com Biochem Physiol* **3**, 227-235.

Cruz, M. J., Sourial, M. M., Treberg, J. R., Fehsenfeld, S., Adlimoghaddam, A. and Weihrauch, D. (2013). Cutaneous nitrogen excretion in the African clawed frog Xenopus laevis: effects of high environmental ammonia (HEA). *Aquat Toxicol* **136-137**, 1-12.

Dames, P., Zimmermann, B., Schmidt, R., Rein, J., Voss, M., Schewe, B., Walz, B. and Baumann, O. (2006). cAMP regulates plasma membrane vacuolar-type H+-ATPase assembly and activity in blowfly salivary glands. *Proc Natl Acad Sci U S A* **103**, 3926-31.

Donini, A. and O'Donnell, M. J. (2005). Analysis of Na+, Cl-, K+, H+ and NH4+ concentration gradients adjacent to the surface of anal papillae of the mosquito Aedes aegypti: application of self-referencing ion-selective microelectrodes. *J Exp Biol* **208**, 603-10.

Endeward, V., Cartron, J. P., Ripoche, P. and Gros, G. (2008). RhAG protein of the Rhesus complex is a CO2 channel in the human red cell membrane. *FASEB J* **22**, 64-73.

Ermak, T. H. and Eakin, R. M. (1976). Fine structure of the cerebral and pygidial ocelli in Chone ecaudata (Polychaeta: Sabellidae). *Journal of Ultrastructure Research* **54**, 243-260.

Evans, D. H., K.J., M. and Robbins, S. L. (1989). Modes of ammonia transport across the gill epithelium of the marine teleost fish *Opsanus beta J Exp Biol* **144**, 339-356.

Fanelli, G. M. and Goldstein, L. (1964). Ammonia excretion in the neotenous newt, *Necturus maculosus* (Rafinesque) *Com Biochem Physiol* **13**, 193-204.

Fehsenfeld, S. and Weihrauch, D. (2012). Differential acid-base regulation in various gills of the green crab *Carcinus maenas*: Effects of elevated environmental pCO2. . *Com Biochem Physiol. A* **164**, 54-65.

Fehsenfeld, S. and Weihrauch, D. (2016). Mechanisms of acid–base regulation in seawater-acclimated green crabs (*Carcinus maenas*). *Can J Zool* **94**, 95–107.

Fransen, M. E. (1988). Coelomic and vascular system. In: The ultrastructure of Polychaeta. *Microfauna Marina* **4**, 199-213.

Gardiner, S. L. (1988). Respiratory and feeding appendages. In: The ultrastructure of Polychaeta. *Microfauna Marina* **4**, 37-43.

Gardiner, S. L. (1992). Polychaeta: General organization, integument, musculature, coelom and vascular system. In *Microscopic Anatomy of invertebrates*, vol. 7 Annelida eds. F. W. Harrisson and S. L. Gardiner). New York: Wiley-Liss.

Goldmann, R. and Rottenberg, H. (1973). Ion distribution in lysosomal suspensions. *FEBS Lett* **33**, 233-238.

Harris, J. L., Maguire, G. B., Edwards, S. and Hindrum, S. M. (1998). Effect of ammonia on the growth rate and oxygen consumption of juvenile greenlip abalone, Haliotis laevigata Donovan. *Aquaculture* **160**, 259-272.

Hausen, H. (2005). Comparative structure of the epidermis in polychaetes (Annelida). *Hydrobiologia* **535/536**, 25-35.

Hu, M. Y., Lee, J. R., Lin, L. Y., Shih, T. H., Stumpp, M., Lee, M. F., Hwang, P. P. and Tseng, Y. C. (2013). Development in a naturally acidified environment: Na+/H+-exchanger 3-based proton secretion leads to CO2 tolerance in cephalopod embryos. *Front Zool* **10**, 51.

Kulkarni, G. K., Kulkarni, V. D. and Rao, A. B. (1989). Nephridial excretion of ammonia and urea in the freshwater leech, *Poecilobdella viridis* as a function of temperature and photoperiod. *Proc. Indian natn. Sci. Acad.* **B55**, 345-352.

Kustu, S. and Inwood, W. (2006). Biological gas channels for NH3 and CO2: evidence that Rh (Rhesus) proteins are CO2 channels. *Transfus Clin Biol* **13**, 103-10.

Larsen, E. H., Deaton, L. E., Onken, H., O'Donnell, M., Grosell, M., Dantzler, W. H. and Weihrauch, D. (2014). Osmoregulation and excretion. *Compr Physiol* **4**, 405-573.

Le Moullac, G. and Haffner, P. (2000). Environmental factors affecting immune responses in Crustacea. *Aquaculture* **191**, 121-131.

Ludewig, U., von Wiren, N. and Frommer, W. B. (2002). Uniport of NH4+ by the root hair plasma membrane ammonium transporter LeAMT1;1. *J Biol Chem* **277**, 13548-55.

Mangum, C. P., Dykens, J. A., Henry, R. P. and Polites, G. (1978). The excretion of NH4+ and its ouabain sensitivity in aquatic annelids and molluscs. *J. Exp. Zool.* **203**, 151-157.

Martin, M., Fehsenfeld, S., Sourial, M. M. and Weihrauch, D. (2011). Effects of high environmental ammonia on branchial ammonia excretion rates and tissue Rh-protein mRNA expression levels in seawater acclimated Dungeness crab Metacarcinus magister. *Comp Biochem Physiol A Mol Integr Physiol* **160**, 267-77.

Masui, D. C., Furriel, R. P., McNamara, J. C., Mantelatto, F. L. and Leone, F. A. (2002). Modulation by ammonium ions of gill microsomal (Na+,K+)-ATPase in the swimming crab Callinectes danae: a possible mechanism for regulation of ammonia excretion. *Comp Biochem Physiol C Toxicol Pharmacol* **132**, 471-82.

Menendez, A., Arias, J. L., Tolivia, D. and Alvarez-Uria, M. (1984). Ultrastructure of gill epithelial cells of Diopatra neapolitana (Annelida, Polychaeta). *Zoomorphology* **104**, 304-309.

Nakada, T., Westhoff, C. M., Kato, A. and Hirose, S. (2007). Ammonia secretion from fish gill depends on a set of Rh glycoproteins. *FASEB J* **21**, 1067-74.

Nawata, C. M., Hirose, S., Nakada, T., Wood, C. M. and Kato, A. (2010). Rh glycoprotein expression is modulated in pufferfish (Takifugu rubripes) during high environmental ammonia exposure. *J Exp Biol* **213**, 3150-60.

O'Donnell, M. J. (1997). Mechanisms of excretion and ion transport in invertebrates. In *Comparative Physiology*, (ed. W. H. Dantzler), pp. 1207-1289. New York: Oxford University Press.

Panz, M., Vitos-Faleato, J., Jendretzki, A., Heinisch, J. J., Paululat, A. and Meyer, H. (2012). A novel role for the non-catalytic intracellular domain of Neprilysins in muscle physiology. *Biol Cell* **104**, 553-68.

Perry, S. F., Braun, M. H., Noland, M., Dawdy, J. and Walsh, P. J. (2010). Do zebrafish Rh proteins act as dual ammonia-CO2 channels? *J Exp Zool A Ecol Genet Physiol* **313**, 618-21.

Pitts, R. J., Derryberry, S. L., Jr., Pulous, F. E. and Zwiebel, L. J. (2014). Antennal-expressed ammonium transporters in the malaria vector mosquito Anopheles gambiae. *PLoS One* **9**, e111858.

Purschke, G., Bleidorn, C. and Struck, T. (2014). Systematics, evolution and phylogeny of Annelida – a morphological perspective. *Memoirs of Museum of Victoria* **71**, 247-269

Quijada-Rodriguez, A. R., Treberg, J. R. and Weihrauch, D. (2015). Mechanism of ammonia excretion in the freshwater leech Nephelopsis obscura: characterization of a primitive Rh protein and effects of high environmental ammonia. *Am J Physiol Regul Integr Comp Physiol* **309**, R692-705.

Reitze, M. a. S., U. (1989). The time dependence of adaption to reduced salinity in the lugworm Arenicola marina L. (Annelida: Polychaeta). *Com Biochem Physiol Part A: Physiology* **93**, 549-559.

Riestenpatt, S., Onken, H. and Siebers, D. (1996). Active absorption of Na+ and Cl- across the gill epithelium of the shore crab Carcinus maenas: voltage-clamp and ion-flux studies. *J Exp Biol* **199**, 1545-54.

Rouse, G. W. and Pleijel, F. (2001). Polychaetes. New York: Oxford University Press, Oxford.

Smith, P. R. (1992). Excretory System. In *Microscopic Anatomy of invertebrates*, vol. 7 Annelida eds. F. W. Harrisson and S. L. Gardiner), pp. 71-108. New York: Wiley-Liss.

Soupene, E., Inwood, W. and Kustu, S. (2004). Lack of the Rhesus protein Rh1 impairs growth of the green alga Chlamydomonas reinhardtii at high CO2. *Proc Natl Acad Sci U S A* **101**, 7787-92.

Storch, V. and Alberti, G. (1978). Ultrastructural observations on the gills of polychaetes. *Helgoländer wissenschaftliche Meeresuntersuchungen* **31**, 169-179.

Tillinghast, E. K. (1967). Excretory pathways of ammonia and urea in the earthworm Lumbricus terrestris L. *J. Exp. Zool.* **166**, 295-300.

Tillinghast, E. K., O'Donnell, R., Eves, D., Calvert, E. and Taylor, J. (2001). Water-soluble luminal contents of the gut of the earthworm Lumbricus terrestris L. and their physiological significance. *Comp Biochem Physiol A Mol Integr Physiol* **129**, 345-53.

Tresguerres, M., Parks, S. K., Salazar, E., Levin, L. R., Goss, G. G. and Buck, J. (2010). Bicarbonate-sensing soluble adenylyl cyclase is an essential sensor for acid/base homeostasis. *Proc Natl Acad Sci U S A* **107**, 442-7.

Weihrauch, D., Becker, W., Postel, U., Riestenpatt, S. and Siebers, D. (1998). Active excretion of ammonia across the gills of the shore crab *Carcinus maenas* and its relation to osmoregulatory ion uptake. *J Comp Physiol [B]* **168**, 364-376.

Weihrauch, D., Becker, W., Postel, U., Luck-Kopp, S. and Siebers, D. (1999). Potential of active excretion of ammonia in three different haline species of crabs. *J Comp Physiol B* **169**, 25-37.

Weihrauch, D., Chan, A. C., Meyer, H., Doring, C., Sourial, M. M. and O'Donnell, M. J. (2012). Ammonia excretion in the freshwater planarian Schmidtea mediterranea. *J Exp Biol* **215**, 3242-3253.

Weihrauch, D., Donini, A. and O'Donnell, M. J. (2011). Ammonia transport by terrestrial and aquatic insects. *J Insect Physiol* **58**, 473-487.

Weihrauch, D., Morris, S. and Towle, D. W. (2004). Ammonia excretion in aquatic and terrestrial crabs. *J Exp Biol* **207**, 4491-504.

Weihrauch, D. and O'Donnell, M. J. (2015). Links between Osmoregulation and Nitrogen-Excretion in Insects and Crustaceans. *Integr Comp Biol* **55**, 816-29.

Weihrauch, D., Wilkie, M. P. and Walsh, P. J. (2009). Ammonia and urea transporters in gills of fish and aquatic crustaceans. *J Exp Biol* **212**, 1716-30.

Weihrauch, D., Ziegler, A., Siebers, D. and Towle, D. W. (2002). Active ammonia excretion across the gills of the green shore crab *Carcinus maenas*: participation of Na(+)/K(+)-ATPase, V-type H(+)-ATPase and functional microtubules. *J Exp Biol* **205**, 2765-75.

Weng, X. H., Huss, M., Wieczorek, H. and Beyenbach, K. W. (2003). The V-type H(+)-ATPase in Malpighian tubules of Aedes aegypti: localization and activity. *J Exp Biol* **206**, 2211-9.

Westheide, W. (1997). The direction of evolution within the Polychaeta. *Journal of Natural History 31, 1-15* **31**

1-15.

Wood, C. M., Munger, R. S. and Toews, D. P. (1989). Ammonia, urea and H^+ distribution and the evolution of ureotelism in amphibians. *J Exp Biol* **144**, 215-233.

Wright, P. A. (1995). Nitrogen excretion: three end products, many physiological roles. *J Exp Biol* **198**, 273-81.

Wright, P. A. and Wood, C. M. (2009). A new paradigm for ammonia excretion in aquatic animals: role of Rhesus (Rh) glycoproteins. *J Exp Biol* **212**, 2303-12.

Young-Lai, W. W., Charmantier-Daures, M. and Charmantier, G. (1991). Effect of ammonia on survival and osmoregulation in different life stages of the lobster Homarus americanus. *Mar Biol* **205**, 293-300.

Table 1: Primers employed in qPCR targeting GAPDH, Na^+/K^+-ATPase (NKA; α-subunit), V-type H^+-ATPase (HAT; subunit B), Rhesus (Rh)-like ammonia transporter (EcRhp1b), EcAMT1, EcAMT3, and EcAMT4 from the marine polychaete, *Eurythoe complanata*.

Gene	Sense primer 5' → 3'	Antisense primer 5' → 3'	Product size (bp)	Reference GenBank
GAPDH	CATCATTCCTGCATCCACTG	ATACTGCTATGCGTGTCCCC	267	KX421092
NKA	GACAACACTGTGATGGGACG	AGAACGACACACCCAGGAAC	133	KX421091
HAT	TCCCTGACTTGACGGGTTAC	GGATACATCAGCGTGGTCCT	164	KX421094
CA-2	ACGGACCTGATGTCCAAGAC	TCCAACTGTGCCTCTGACAC	197	KX421093
EcRhp1b	GTGTTTGGGGCATACTTTGG	ACACCCAGAGGAAGACGGTA	133	KX421088
EcAMT1	TCAGCTGTCTCAAATGCAGAA	GTTGGTGGTGTTTTTGCTCC	151	KX458239
EcAMT3	GCGGCGGTATCTACTGTCAT	ATGTGACAGACACAAGGGCA	136	KX421089
EcAMT4	TGGATATCGCAATTGGTTCA	CTTGATATGCCAAGCCCAAT	205	KX421090

Table 2: Absolute mRNA expression levels (fg cDNA/50 ng total RNA) of Na^+/K^+-ATPase α-subunit (NKA), V-type H^+-ATPase subunit B (HAT), Carbonic anhydrase isoform 2 (CA-2), Rh-like protein EcRhp1b, EcAMT1, EcAMT3 and EcAMT4 in the marine polychaete *Eurythoe complanata*.

	NKA	HAT	CA-2	EcRhp1b	EcAMT1	EcAMT3	EcAMT4
Gills							
Mean	1.0	0.1	1.44	2.1	0.013	0.43	8.5
SEM	0.12	0.025	0.23	0.2	0.004	0.08	2.2
N	4	5	4	5	5	5	5
Body							
Mean	0.37	0.025	0.25	0.72	0.0004	0.14	0.76
SEM	0.14	0.0028	0.06	0.19	0.00011	0.05	0.32
N	4	4	4	4	5	5	4

Figures

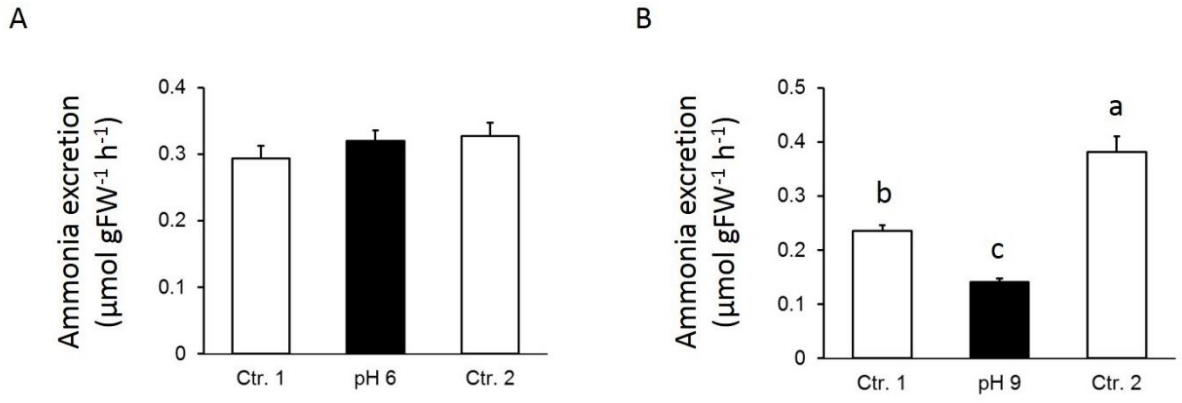

Figure 1: Ammonia excretion rates (means ± SEM) in *E. complanata* exposed to different pH regimes. Ammonia excretion rates were sampled in three consecutive hours. In the 2nd sampling period the seawater was either adjusted to pH 6 (A, closed bar) or pH 9 (B, closed bar). Significant differences are indicated by different letters. Data were analyzed employing a one-way Anova with repeated measures using a Tukey's pairwise comparison; n= 4.

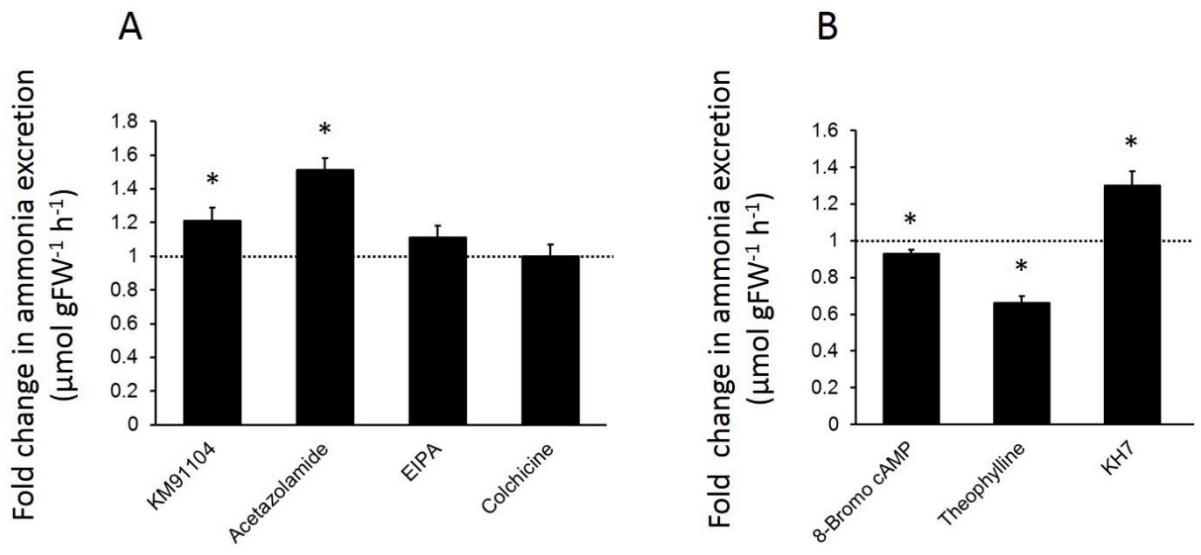

Figure 2: Effects of different inhibitors (A) and modulators of cellular cAMP levels (B) on ammonia excretion rates (means ± SEM) in *E. complanata*. Control values for each treatment were set to 1 (dotted line), with values measured under the influence of the agents are given as fold of the respective control. The concentrations and target of the pharmacological agents (in brackets) were: KM91104 (V-ATPase; 5 µmol l^{-1}; n=4); acetazolamide (carbonic anhydrase; 2 mmol l^{-1}, n=4); EIPA (cation/H^+-exchanger; 100 µmol l^{-1}, n=4); colchicine (microtubules network; 0.5 mmol l^{-1}, n=4), 8-Bromo-cAMP (intracellular cAMP levels; 25 µmol l^{-1}, n=4), Theophylline (phosphodiesterase; 1 mmol l^{-1}, n=4), KH7 (soluble adenylyl cyclase; 10 µmol l^{-1}, n=4). Significant differences from the respective control values are indicated by "*". Data were analyzed employing a paired student's t-test (two-tailed) on excretion rates prior to calculation of fold-change values.

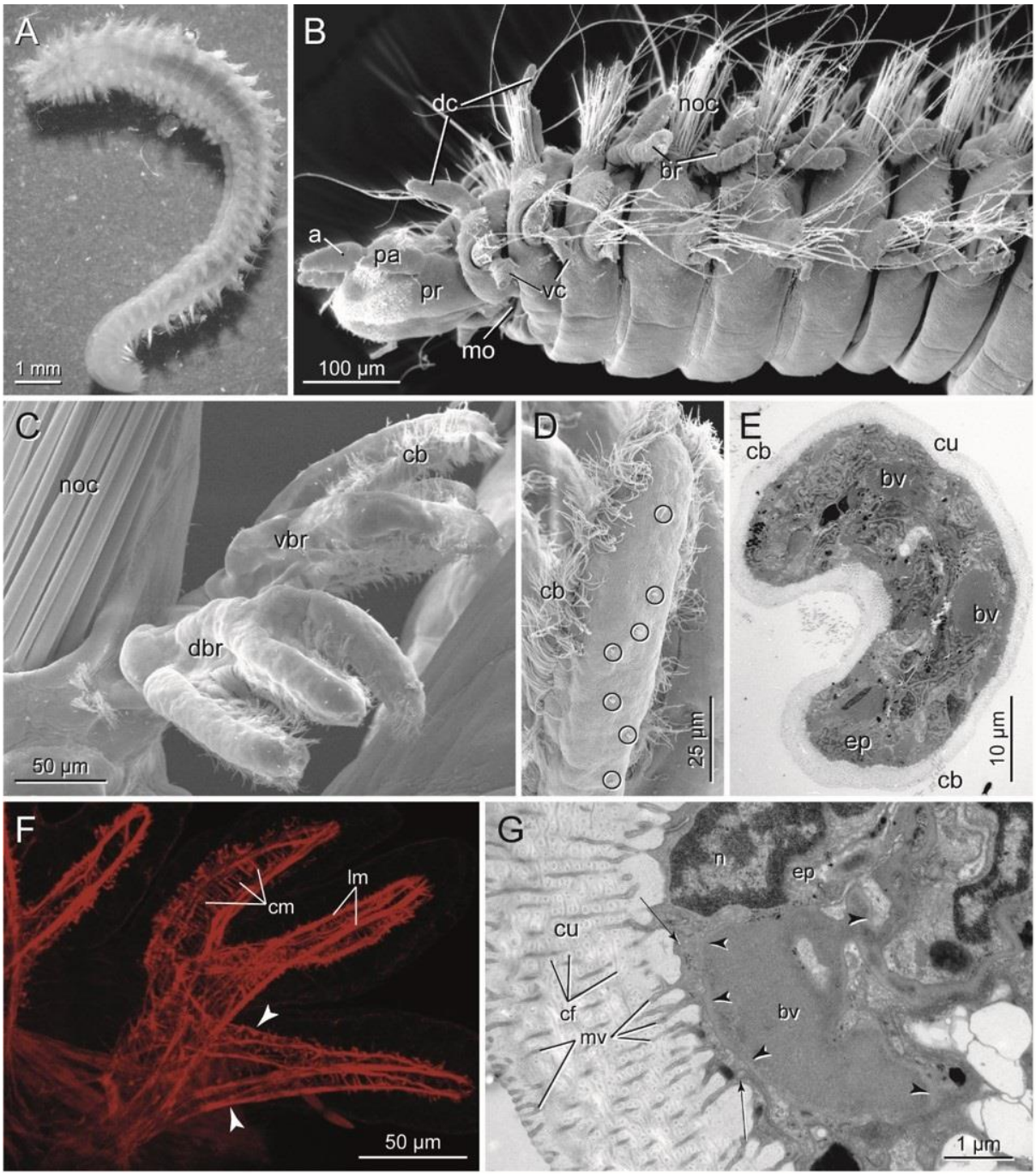

Figure 3: Morphology and position of branchiae in *E. complanata*. A) LM; B-D) SEM; E, G) TEM; F) cLSM. A) Entire living animal; LM. B) Anterior end in lateral view showing parapodia with dorsal (dc) and ventral cirri (vc) and branchiae (br) well protected between

notochaetae (noc); a, antenna; mo, mouth; pa, palp; pr, prostomium. C) Enlargement of single branchia branching into dorsal (dbr) and ventral (vbr) group of branchial filaments; each filament with ciliary band (cb) on narrow side; noc, notochaetae. D) Enlargement of a single branchial filament with continuous ciliary band (cb) surrounding entire filament, receptor cell cilia encircled. E) Low power TEM micrograph showing entire branchial branch in cross section with ciliary bands (cb), blood vessels (bv), epidermis (ep) and thin cuticle (cu). F) Branchia stained with phalloidin against actin (red), each branch is supplied with intrinsic musculature. Musculature of branchiae composed of strong longitudinal (lm) and fine circular fibers (cm) following course of blood vessels forming a hairpin (arrowheads). G) Blood space (bv) and connection to deeper regions through spaces in ECM; arrowheads point to continuous ECM surrounding the blood; arrows point to thin epidermal cover measuring between 130 - 350 nm. Cuticle (cu) on branchia traversed and extended by branching microvilli (mv); collagen fibers (cf) form loose network

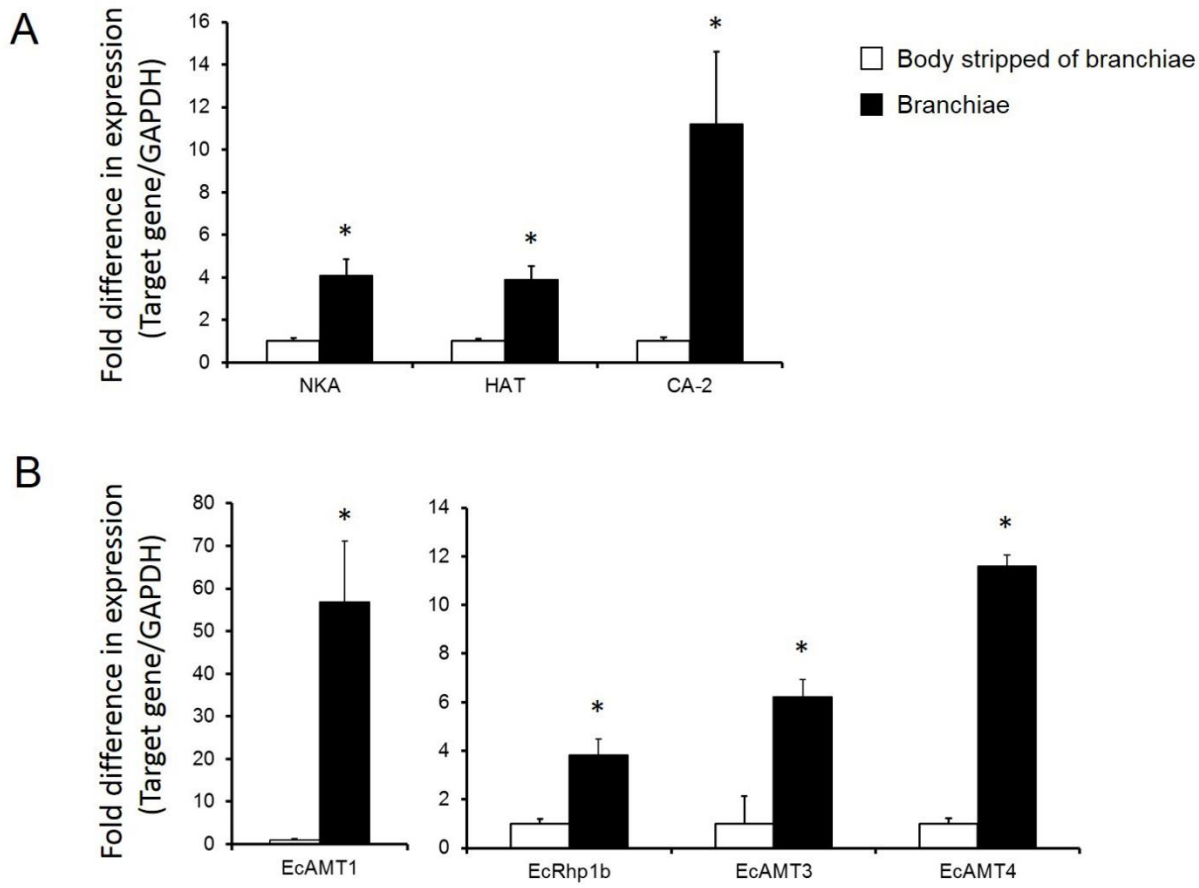

Figure 4: Fold difference in relative mRNA expression levels (means ± SEM) detected in the body (set to 1, open bars) and the branchiae (closed bars) in *E. complanata*. A) NKA (Na^+/K^+-ATPase α-subunit, n=4), HAT (subunit B, V-type H^+-ATPase, n=4), CA-2 (cytoplasmatic carbonic anhydrase 2, n=4). B) EcAMT1 (n=4), EcRhP1b (n=4), EcAMT3 (n=4), and EcAMT4 (n=4). The asterisk (*) indicates significant differences between the relative expression levels in the body and the branchiae. Data were analyzed employing a paired student's t-test (two-tailed) on expression prior to calculation of fold-change values.

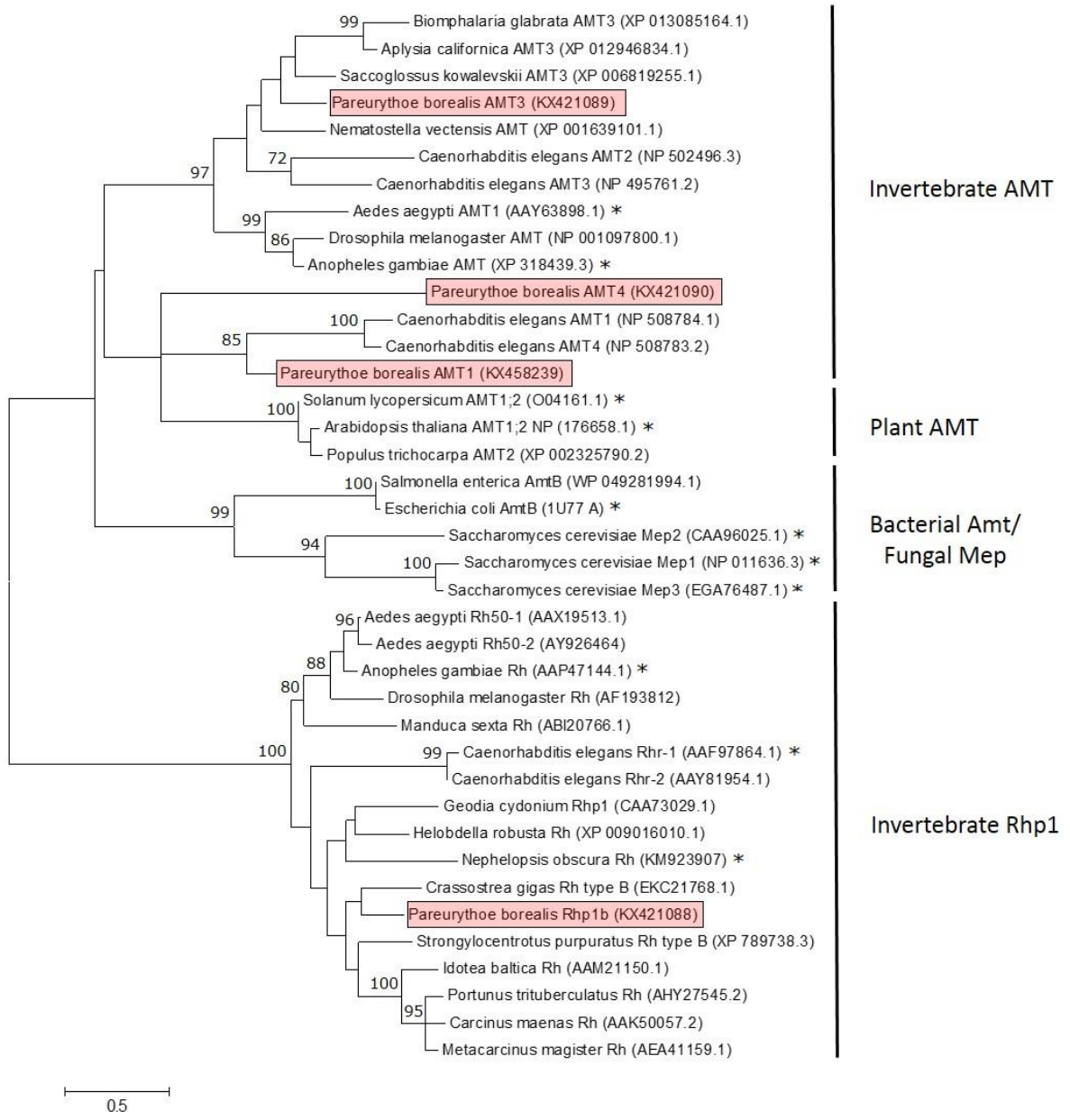

Figure 5: Phylogenetic analysis of putative *E. complanata* Rh protein and AMTs. Numbers beside branches represent bootstrap values from 1000 replicates. The tree branches are drawn to scale, with the scale bar representing the number of amino acid substitutions per site. * denotes sequences with a confirmed ammonia transport capability. The black box indicates *E.*

complanata sequences. GenBank accession numbers are given in brackets following the species name and gene.

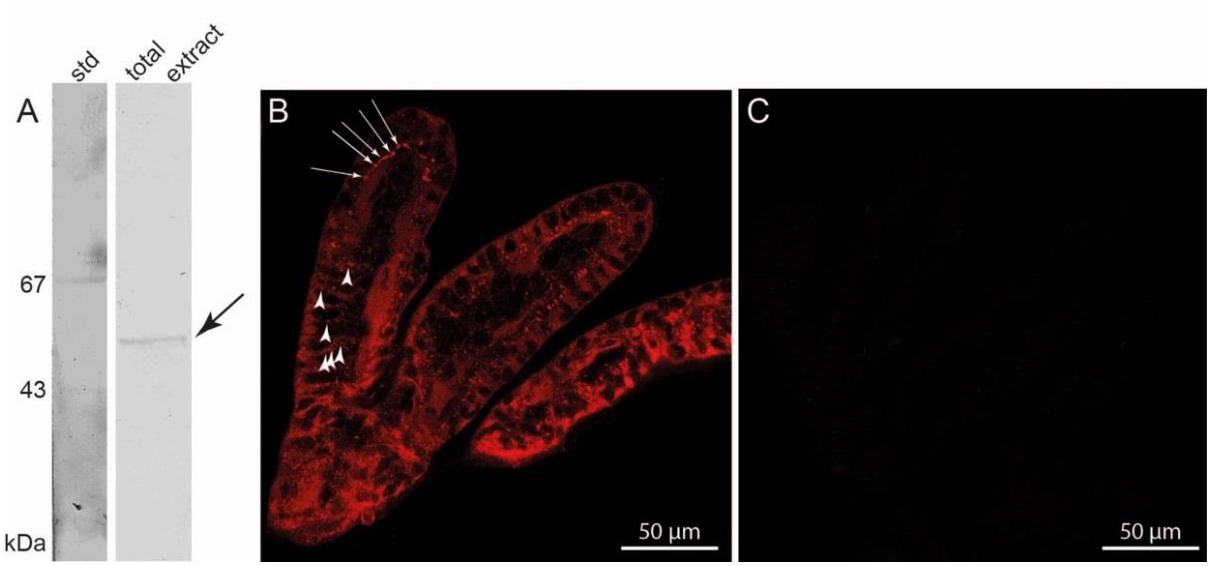

Figure 6: Immunolocalization of the V-type H^+-ATPase in branchiae of adult *E. complanata*. A) Western blot of total protein extract isolated from adult *E. complanata*. Application of anti-V-ATPase antibodies (subunit B specific) results in detection of a single protein of about 55 kDa (arrow). B) Application of the same antibodies to parapodial appendice tissue results in detection of the V-type H^+-ATPase mainly in basolateral membranes (arrows). An additional signal is obvious in vesicular structures within the cytoplasm (arrow heads). C) Control staining, lacking the primary antibody. No signal above background was observed.

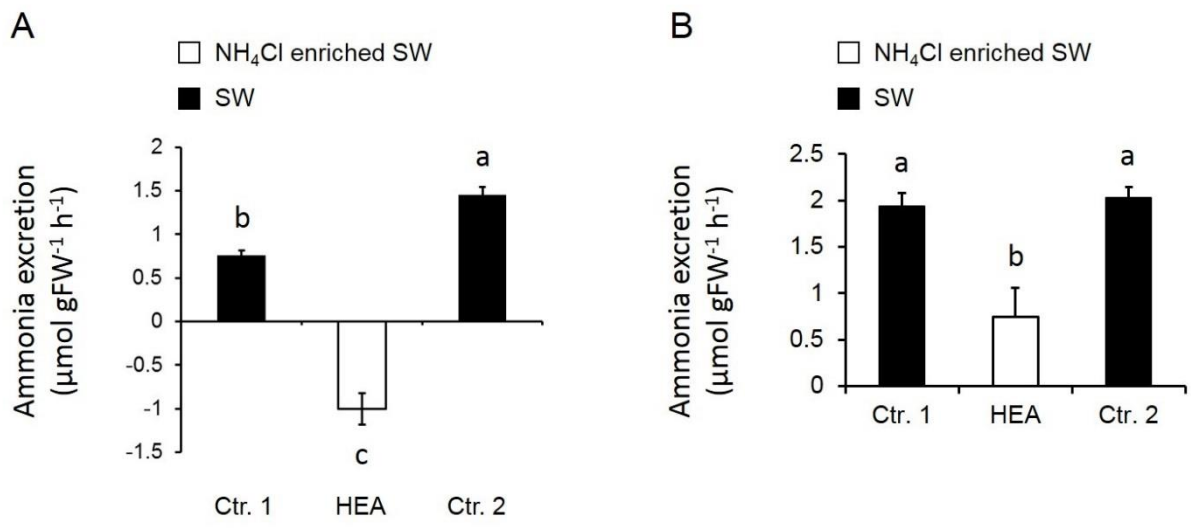

Figure 7: Ammonia excretion rates in A) *E. complanata* acclimated to seawater (SW) and B) animals acclimated to seawater (SW) enriched with 1 mmol l^{-1} NH_4Cl (HEA) (means ± SEM). Closed bars represent exposure to SW, open bars exposure to SW enriched with 1 mmol l^{-1} NH_4Cl. Significant differences are indicated by different letters. Data were analyzed employing a one-way Anova with repeated measures using a Tukey's pairwise comparison; n= 4.

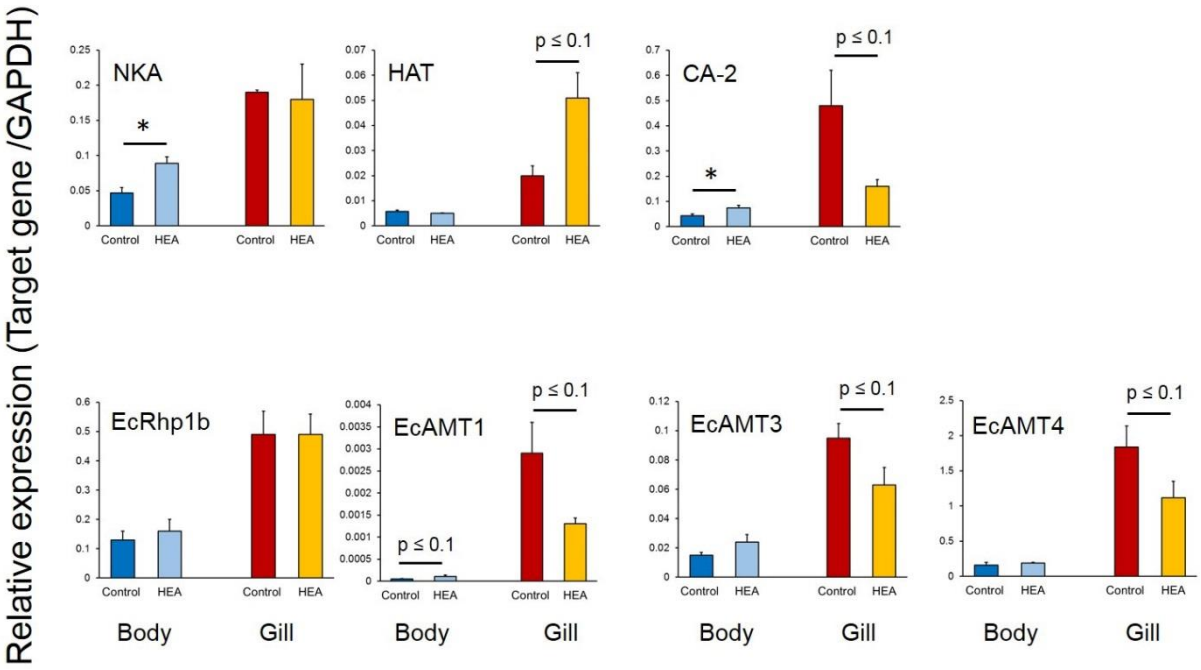

Figure 8: Relative mRNA expression of target proteins in the body (dark and light blue bars) and branchiae (red/orange bars) in SW and HEA (1 mmol l^{-1} NH_4Cl) acclimated *E. complanata* (means ± SEM). NKA, Na^+/K^+-ATPase α-subunit (n=4-5); HAT, V-type H^+-ATPase subunit B (n= 4); CA-2, cytoplasmatic carbonic anhydrase (n=4-5); EcAMT1 (n=4); EcRhp1b (n-4-5); EcAMT3 (n=5); EcAMT4 (n=4-5). Significant differences between control and HEA acclimated animals are indicated by "*". A p-value between 0.05 and 0.1 (trending; in tendency) is indicated by $p \leq 0.1$. Data were analyzed employing an unpaired student's t-test (two-tailed).

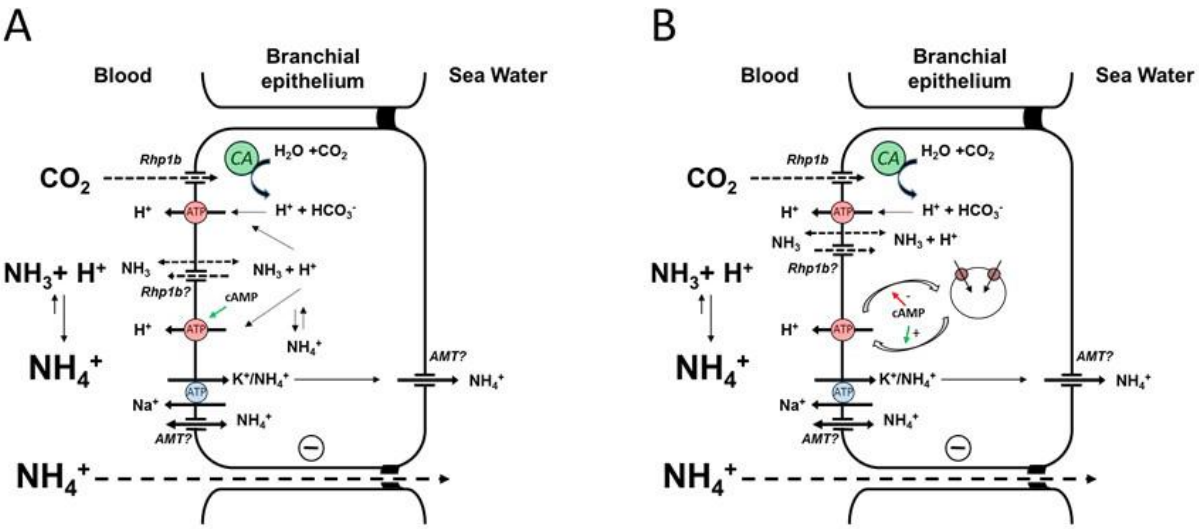

Figure 9: Hypothetical working models of the ammonia transport pathways in the branchiae of *E. complanata*. For the description of the pathways please refer to the text. CA, cytoplasmatic carbonic anhydrase; "?" indicates speculative localization of transporter; the green arrow indicates indirect activation of V-type H^+-ATPase *via* cAMP or insertion of V-type H^+-ATPase carrying vesicles. Arrows with dotted lines indicate a diffusive pathway of a gas or the paracellular diffusion.